2013 IEEE/RSJ International Conference on
Intelligent Robots and Systems (IROS)
November 3-7, 2013. Tokyo, Japan

Perforation Risk Detector Using Demonstration-based Learning for Teleoperated Robotic Surgery

Takayuki Osa[1], Takuto Haniu[1], Kanako Harada[1], Naohiko Sugita[1] and Mamoru Mitsuishi [1]

Abstract— **Loss of haptic sensation in a master-slave system is one of the open problems in robotic surgery, and recognition of surgical situations through haptic sensation is a challenge. In this paper we propose an autonomous risk-detection system for a master-slave surgical robotic system in order to estimate a property of an object (i.e., contact impedance) using a force sensor mounted on a surgical robotic instrument. The system autonomously detects the risk based on the estimated contact impedance and accordingly activates the motion at the slave unit as well as the force feedback at the master unit. We implemented the proposed method in a teleoperated master-slave system to detect the perforation risk of a membranous object. The performance of the system was evaluated through experiments. The classification accuracy for perforation risk was about 98.5 % in fourfold cross-validation. The experiments verified that the risk detection system accurately detected the perforation risk and improved the safety of the master-slave system.**

I. INTRODUCTION

Robotic surgery has attained great success in recent years. The number of clinical reports on robotic surgery has been increasing, and the application range of robotic surgery has been extended in the last decade [1].

Some of the most successful robotic surgical systems are master-slave systems such as the da Vinci Surgical System (Intuitive Surgical Inc., CA, USA) [2]. The master-slave configuration can enhance the maneuverability of robotic surgical instruments that are long and thin, but the surgeon cannot have a direct haptic sense in master-slave robotic surgery. To provide haptic information and enhance the robotic operability, force feedback systems have been developed for robotic surgery [3], [4], [5]. Most of these systems employ constant force feedback gains, regardless of the surgical situation. Although these systems have shown the efficacy of force feedback, the haptic information available in robotic surgery is unnatural and unsatisfactory for recognition of surgical situations online. As we discussed in our previous papers [6], [7], a force feedback system will enhance haptic sensation and improve the safety of a surgical operation by adaptively controlling force feedback gains according to the surgical situation.

This work was supported in part by the Global COE Program, Global Center of Excellence for Mechanical Systems Innovation by the Ministry of Education, Culture, Sports, Science and Technology and Grant-in-Aid for Scientific Research(S) 23226006.

[1]T. Osa, T. Haniu, K. Harada, N. Sugita and M. Mitsuishi are with Department of Mechanical Engineering, the University of Tokyo, 7-3-1 Hongo Bunkyoku Tokyo, 113-8656 Japan, (Phone: +81-3-5841-6357; fax:+81-3-5841-6357; e-mail: osa, haniu, kanako, sugi, mamoru@nml.t.u-tokyo.ac.jp).

In another line of research, haptic exploration systems for robotic surgery have been investigated by many researchers [8], [9], [10]. Such systems could convey a great deal of useful information to surgeons during surgical operation, such as that obtained by palpation. However, these previous studies mainly focused on estimating the property of objects. Therefore, a way to exploit the benefit of haptic exploration needs to be investigated.

In this paper, we propose to use the estimated property of objects to recognize the surgical situation and combine it with automatic robotic control to improve the safety of surgical operations. Specifically, we developed a system that not only detects the risk of perforating a membranous object by learning from preoperative demonstrations but also autonomously activates motion at a slave unit and force feedback at a master unit. The system estimates the contact state between an object and a surgical instrument to detect the risk of perforation. Activation of the force feedback serves to alert the perforation risk, and when the detected risk is high, the system autonomously stops the execution of motion signals received from the master unit.

In surgical operations, palpations are often performed to identify the diseased part of an organ, a task which is sometimes difficult. For instance, palpation to identify the locations of arteries beneath opaque tissue or those of lung cancer is necessary in the scenarios of robotic minimally invasive surgery [11], [12]. However, palpation could lead to perforation of organs in the event of human errors or operational mistakes. The system developed here can be used to improve the safety of such surgical procedures.

The rest of this paper is structured as follows: The next section presents an overview of the proposed method and the details of the proposed algorithm. Section III describes experiments conducted to evaluate the developed system. The last section concludes this study and outlines of the future work.

II. METHOD

A. Overview of the Proposed Method

An overview of the proposed system is shown in Fig. 1. The force detected at the tip of a robotic surgical instrument is used to estimate the contact impedance of the membranous object handled by the instrument. In preoperative preparation, the system learns the risk of perforation from demonstrations. The online system estimates a property of an object, specifically the contact impedance of the object, and detects the perforation risk using the learned model. The robotic system autonomously activates the motion at the slave unit and the

978-1-4673-6357-0/13/$31.00

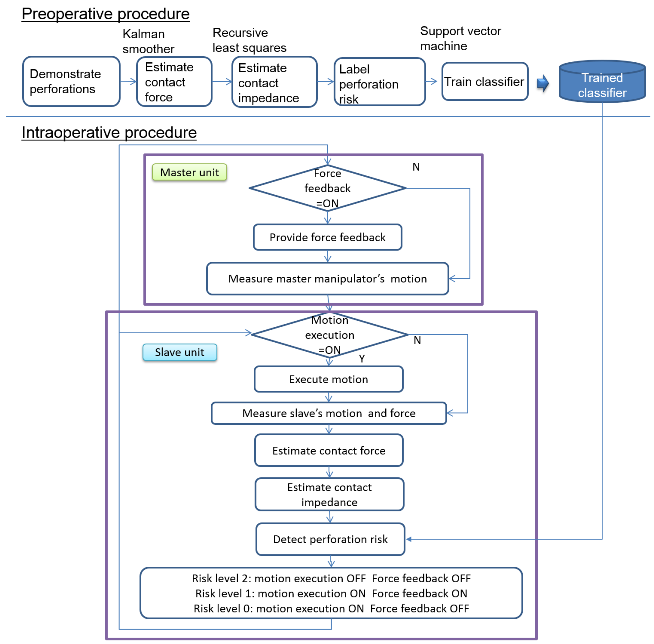

Fig. 1. A diagram of the proposed control system.

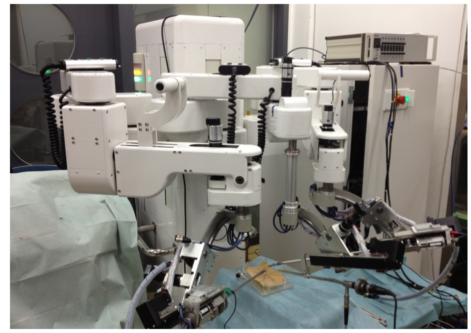

Fig. 2. The slave unit with three robotic arms.

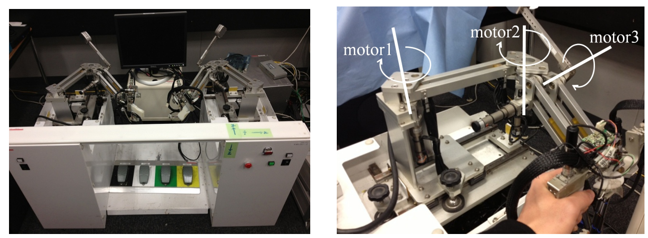

(a) (b)

Fig. 3. The master unit. (a) Master manipulators. (b) Master manipulator with three motors to exert 3 DOF force feedback.

force feedback at the master unit, according to the estimated risks.

In the preoperative preparation, we employ a demonstration-based learning. We assume that the object handled with the robotic surgical instrument is known and the model for estimating the contact impedance of the object is available in advance. During the demonstrations, an operator pushes and perforates the membranous object. The contact force, the motion of the surgical instrument, and the pushing depth are recorded. The developed system detects the perforation risk using a support vector machine (SVM). To obtain the input vectors of the SVM, the measured contact force is smoothed with a Kalman smoother and the contact impedance at each sampling time is estimated using recursive least squares (RLS). The motion of the robotic surgical instrument, the estimated contact impedance, and the measured contact force are used as feature vectors for training the SVM. Each feature vector is given a label corresponding to perforation risk based on the perforating force estimated in each demonstration.

During an intraoperative procedure, the contact force is estimated by the Kalman smoother, and the contact impedance of the object is estimated by RLS in the same manner as during the preoperative procedure. Using those estimated parameters, the perforation risk is detected by the SVM in real time. According to the outputs of the SVM, the robotic system automatically activates the motion at the slave site and the force feedback at the master site. This control system framework is applicable to any other master-slave system with force sensing capabilities.

We implemented the proposed method in a master-slave system for teleoperated surgery [7], [13], [14]. The system consists of a master unit and a slave unit (see Fig. 3). The slave robot has three robotic arms on which two robotic surgical instruments and one laparoscope are attached. On each robotic surgical instrument, a force sensor is mounted (see Fig. 4). The force sensor is composed of strain gauges. The measurement range and the accuracy of the force sensor are 0-15 N and 0.2 N, respectively. The master manipulator is capable of applying 20 N at the tip of the robotic surgical instrument.

B. Estimation of Contact Force Using Kalman Smoother

We used the Kalman smoother to filter noises and estimate the actual contact force. The process model is expressed as follows:

$$\begin{bmatrix} f_{k+1} \\ \dot{f}_{k+1} \end{bmatrix} = A \begin{bmatrix} f_k \\ \dot{f}_k \end{bmatrix} + B \begin{bmatrix} \Delta x_k \\ \Delta \dot{x}_k \\ \Delta \ddot{x}_k \end{bmatrix} + w_k \qquad (1)$$

where $A = \begin{bmatrix} 1 & 1 \\ 0 & 1 \end{bmatrix}$, $B = \begin{bmatrix} \bar{k} & \bar{c} & 0 \\ 0 & \bar{k} & \bar{c} \end{bmatrix}$, $w_k \sim N(0, Q)$, f_k is the contact force; x_k, the pushing depth; and Q, the covariance matrix of the process noise. Note that $\bar{k}$ and $\bar{c}$ are estimated coefficients for elasticity and viscosity, respectively. In (1), the motion of the robotic surgical instrument is expressed as a control input. Observation of the contact force is modeled as follows:

$$f_{m,k} = H \begin{bmatrix} f_k \\ \dot{f}_k \end{bmatrix} + v_k \qquad (2)$$

where $f_{m,k}$ is the force measured at the kth measurement, $H = [1, 0]$, f_k is the actual contact force at the kth step, $v_k \sim N(0, R)$ represents the measurement noise, and R is the covariance of the measurement noise. In the Kalman

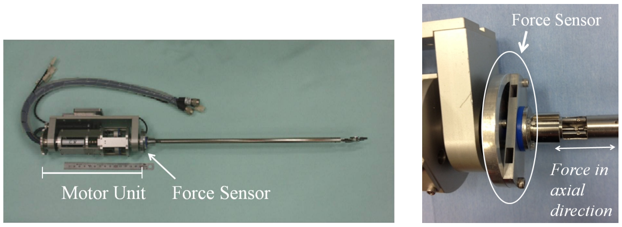

(a) (b)

Fig. 4. The robotic surgical instrument: (a)An overview and (b) the force sensor.

smoother, the process noise and measurement noise are assumed to follow a Gaussian distribution. The details of the Kalman smoother are found in the literature [15].

C. Estimation of Contact Impedance

Many studies related to estimation of the contact impedance of the organs and tissues are found in [16], [8], [9], [10], [17]. Although these studies employed nonlinear models to estimate the mechanical properties of the soft tissue, we used a linear model to express the contact impedance of the object as follows:

$$\Delta f = k\Delta x + c\Delta \dot{x} \tag{3}$$

The reason that we used the linearized model is that coefficients can indicate the deformation of the object. The coefficients vary according to the deformation of the object. Therefore, by learning the changes in the coefficients, the deformation of the object can be estimated.

The RLS method is often used for estimating mechanical properties [16], [8], [9], [10], [17]. We also employed RLS to estimate the contact impedance of the object. In RLS, the following equations are computed recursively:

$$\begin{aligned} K_n &= \frac{P_{n-1}u_n}{\lambda + u_n^T P_{n-1} u_n} \\ W_n &= W_{n-1} + K_n\left(d_n - u_n^T W_{n-1}\right) \\ P_n &= \frac{1}{\lambda}\left(I - K_n u_n^T\right) P_{n-1} \end{aligned} \tag{4}$$

where u is the input vector and d is the desired value. In (4), P_n is initialized as $P_0 = I$. In the proposed method, the input vector was set as $u = [\Delta x, \Delta\dot{x}]^T$ and the desired value was set as $d = \Delta\hat{f}$, where x is the pushing depth, and $\hat{f}$ is the contact force estimated by the Kalman smoother. A forgetting factor λ of less than 1 puts greater weights on the newer measurements. For this system, the value $\lambda = 0.9$ performed well.

D. Perforation Risk Detection

Many researchers have reported on surgical task recognition [18], [19], [20], [21]. Lalys, et al. developed a system with surgical task recognition using video microscopy images [18]. They employed dynamic time warping and a hidden Markov model (HMM) to analyze the sequence of video images. Padoy et al. developed a system for online surgical task recognition in an operating room monitoring [19]. The HMM is often used for surgical task recognition due to its suitablity for modeling time-series data. However, the using an HMM is not suitable for learning nonlinear decision boundary.

Therefore, we employ an SVM for perforation risk detection [22]. We classify the perforation risk using data at every time step. The nonlinear decision boundaries can be learned using the SVM with a kernel trick [23]. We use the C-SVM to tolerate inseparable training data sets. The learning process of the C-SVM can be summarized as the following optimization problem:

$$\min\left\{\frac{1}{2}w + C_k\sum_{i=1}^{l}\xi_i\right\} \tag{5}$$

subject to

$$\begin{aligned} y_i\left(w\cdot x_i - b\right) &\geq 1-\xi_i \\ \xi &\geq 0 \end{aligned} \tag{6}$$

where x_i is a feature vector that represents the state of the system and y_i is the risk level associated with state x_i. ξ_i are called slack variables, which penalize misclassified points. In (5), we used the class values of $[C_0, C_1, C_2] = [1, 1.2, 2]$ where C_i is a class weight associated with the perforation risk i. By assigning the larger class weights to higher risks, we make the classification accuracy of higher risks become more important. We employ a radial basis function (RBF) as a kernel function. The RBF is defined as follows:

$$k\left(x_i, x_j\right) = exp\left(-\gamma\left\|x_i - x_j\right\|^2\right) \tag{7}$$

This kernel trick enables the setting of nonlinear decision boundaries for the perforation risk detector. The details of C-SVM can be found in [22]. We use the coefficients estimated by RLS as the SVM inputs. To avoid risks due to large forces and high-speed motion, we use the feature vector $x_i = [\hat{f}, \Delta\hat{f}, v, a, \hat{k}, \hat{c}]$ where $\hat{f}$ is the contact force estimated by the Kalman smoother, v and a are the linear velocity and acceleration of the surgical instrument and the $\hat{k}$ and $\hat{c}$ are the contact impedance coefficients estimated by RLS.

We label each feature vectors with a risk level based on the force f_p measured at perforation of each demonstration. The risk level r is thus set as follows.

$$\begin{aligned} \hat{f} < \alpha_1 f_p &\Rightarrow r = 0 \\ \alpha_1 f_p \leq \hat{f} \leq \alpha_2 f_p &\Rightarrow r = 1 \\ \alpha_2 f_p \leq \hat{f} &\Rightarrow r = 2 \end{aligned}$$

where $\hat{f}$ is the contact force estimated by the Kalman smoother. The values of α_1 and α_2 determine the margin of safety. For the preliminary experiment, we used the values $[\alpha_1, \alpha_2] = [0.2, 0.4]$. The values need adjustment for each application.

E. Adaptive Control of the Master Manipulator

Based on the outputs of the SVM, the robotic system autonomously activates the master-slave motion and the force feedback as follows:

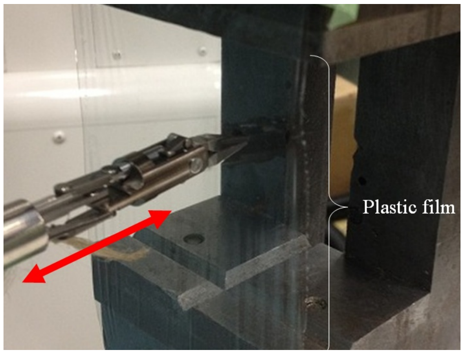

Fig. 5. The setup for the preliminary experiment. The motion of the robotic surgical instrument was constrained to the axial direction as shown by the red arrow.

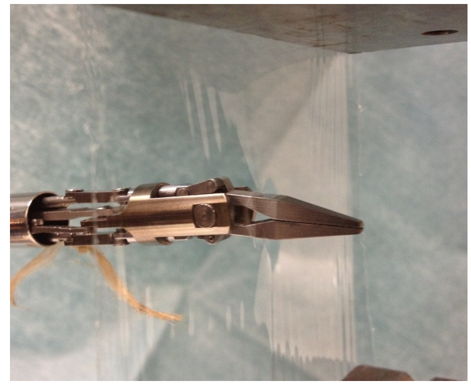

Fig. 6. Perforation of a thin film. An operator perforated the thin plastic film, and the force and motions of the robotic surgical instrument were recorded.

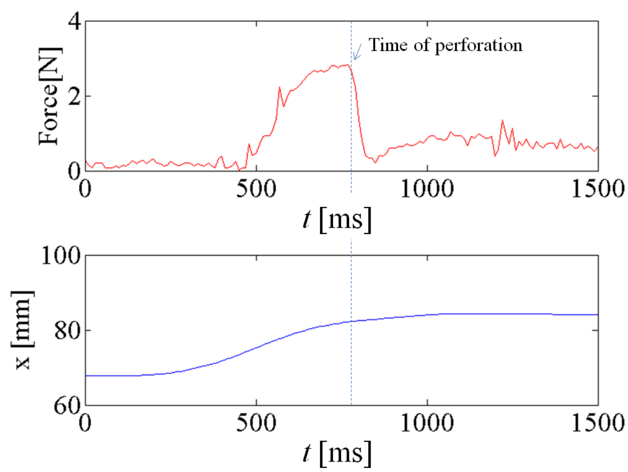

Fig. 7. Examples of the data recorded for training the risk detector. At $t = 780$ ms, the perforation of the film was observed.

RISK LEVEL 0
master-slave motion $\longrightarrow$ ON
force feedback $\longrightarrow$ OFF
RISK LEVEL 1
master-slave motion $\longrightarrow$ ON
force feedback $\longrightarrow$ ON
RISK LEVEL 2
master-slave motion $\longrightarrow$ OFF
force feedback $\longrightarrow$ OFF

When no risk is detected by the system(RISK LEVEL 0), no force feedback is provided. At RISK LEVEL 1, the force feedback is provided to inform the operator of the increased risk of perforation. At RISK LEVEL 2, the slave system autonomously disables the execution of the motion signal received from the master system. An autonomous switching system is implemented in the slave unit to provide robustness against possible communication problems between the master and slave units.

III. Experiments

A. Experimental Setup

We performed a preliminary experiment to evaluate the performance of the proposed method. The experimental setup was designed to simulate the scenario of the palpation of membranous objects by using a robotic surgical system (see Fig. 5). A plastic film with nonlinear contact impedance was used as the membranous object. The film was made from polyvinyl chloride, and its thickness was 8 μm. The operator moved the master manipulator and perforated the plastic film several times with the robotic surgical instrument. The force and motion of the surgical instrument were recorded (see Fig. 6). Only the axial motion of the robotic surgical instrument was used in the experiment. However, the proposed method can be applied to other master-slave systems with multiple degrees of freedom by changing the SVM inputs.

B. Training Data for the Classifier

An example of the data used for SVM training is shown in Fig. 7. At the instant of perforation, the measured force decreased remarkably.

An example of the performance of the Kalman smoother is shown in Fig. 8. The Kalman smoother successfully filtered out the noise, and the processing speed was sufficient for online processing.

An example of the processed datasets is shown in Fig. 9. The contact impedance of the film was successfully estimated. At the instant of perforation, the estimated contact impedance diverged, since the estimated contact force suddenly decreased. Therefore, while training the perforation risk detector, we used only the data before perforation.

C. Cross-Validation of Perforation Risk Detector

In order to validate the performance of the perforation risk detector, we performed a fourfold cross-validation. We performed the perforation experiment eight times and simulated the performance of the perforation risk detector. The results are listed in Table I.

As shown in Table I, the accuracy of classification was nearly 100 % for Risk Levels 0 and 2. However, the accuracy of classification for Risk Level 1 was about 35 %. This classification accuracy represents a trade-off between Risk Levels 1 and 2. In this study, the classification accuracy for

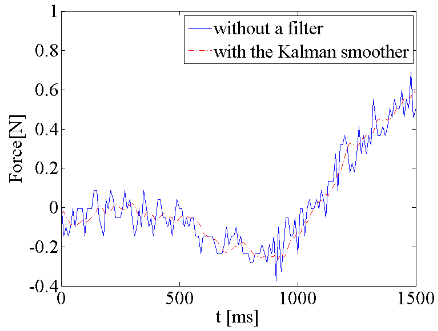

Fig. 8. Performance of the Kalman smoother. The blue solid line represents the raw measurement data of force and the red dash-dot line represents the output of the Kalman smoother.

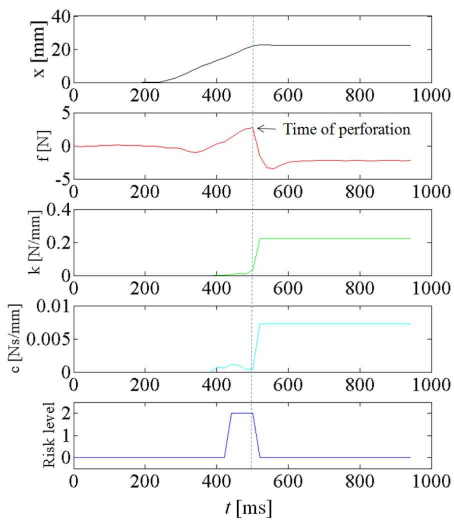

Fig. 9. Example of processed data. In all of the plots, X axis represents time [ms]. At $t = 520$ms, perforation of the film was observed.

Risk Level 2 was more important than that for Risk Level 1.

D. Haptic Exploration Experiment

1) Experimental procedure: In order to demonstrate that the proposed method improves the safety of the master-slave system, we performed an experiment. The subjects were asked to compare the stiffness of two plastic films by touching these with the robotic surgical instrument. In actual surgical operations, surgeons often check the stiffness of the organ by touching it with surgical instruments (so-called haptic exploration), as Tamamoto et al. reported in [8]. Five engineering students participated in the experiment.

TABLE I
RESULTS OF CROSS VALIDATION.

No.	Risk level 0	Risk level 1	Risk level 2
1	99.9% (10466/10467)	42.9% (12/28)	100% (96/96)
2	99.9% (7631/7646)	25.9 % (14/54)	100% (82/82)
3	99.9% (10045/10049)	25.0% (15/60)	94.19% (227/241)
4	99.9% (11592/11593)	45.7% (16/35)	100% (98/98)
Ave.	99.9%	34.9%	98.5 %

TABLE II
RESULTS OF USER EXPERIMENT.

System	Number of perforation
Conventional force feedback system	4/5
The proposed system	1/5

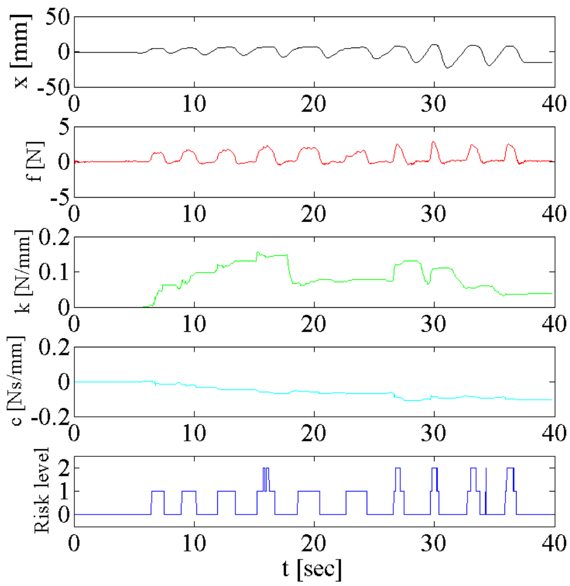

Fig. 10. Recorded data in the experiment using the developed system.

The stiffnesses of the two plastic films in this experiment were the same, but we did not inform the subjects of this fact. The subjects performed the experiment both with the conventional force feedback system and with the developed system. When the developed system was used, the force feedback and motion were activated on the basis of the estimated perforation risk. In contrast, when the conventional force feedback system was used, the force feedback was always provided. In this experiment the laparoscopic image was delayed by 200 ms to simulate communication problems between the master and slave units.

2) Results of the experiment: The results are listed in Table II. When using the conventional force feedback system, four out of five subjects accidentally perforated the plastic film during haptic exploration. However, only one subject perforated the plastic film during the operation with the proposed system. An example of the data recorded during the experiment using the developed system is shown in Fig. 10.

In this experiment, all subjects repeatedly pushed the plastic films with the robotic surgical instrument and checked its deformation while feeling the force feedback to the master manipulator. In the process of comparing the stiffness of the films, subjects paid much more attention to the stiffness and much less attention to perforation risk. Even though the subjects did not pay much attention to perforation risk, only one subject perforated a film in the experiment with the developed system. As shown in Fig. 10, the developed system detected the perforation risk and autonomously terminated the motion once Risk Level 2 was reached. Therefore, we concluded that the developed system would improve the safety of master-slave teleoperated surgery.

IV. CONCLUSION AND FUTURE WORK

The system estimates the contact between an object and a surgical instrument to detect the perforation risk. Using the autonomous risk-detection system, the robotic system autonomously activates the motion at the slave unit and the force feedback at the master unit. We implemented the proposed method in a master-slave teleoperated system to detect the perforation risk of a membranous object. The performance of the system was evaluated through experiments. The experiments verified that the risk detection system accurately detected the perforation risk and improved the safety of the master-slave system.

The current work is done under the assumptions that the object is known, its model for estimating the contact impedance is available, and the contact impedance can be learned by preoperative demonstrations. Therefore, we intend to work on the online identification of objects that do not require preoperative demonstrations and the learning process. In addition, to combine the current method with unsupervised learning of risk detection is potential work.

REFERENCES

[1] C. Ramsay, R. Pickard, C. Robertson, A. Close, L. Vale, N. Armstrong, D. Barocas, C. Eden, C. Fraser, T. Gurung, D. Jenkinson, X. Jia, T. Lam, G. Mowatt, D. Neal, M. Robinson, J. Royle, S. Rushton, P. Sharma, M. Shirley, and N. Soomro., "Systematic review and economic modelling of the relative clinical benefit and cost-effectiveness of laparoscopic surgery and robotic surgery for removal of the prostate in men with localised prostate cancer," *Health Technology Assessment*, vol. vol. 16 no. 41, 2012.

[2] F. W. Mohr, V. Falk, A. Diegeler, T. Walther, J. F. Gummert, J. Bucerius, S. Jacobs, , and R. Autschbach, "Computer-enhanced hrobotich cardiac surgery: experience in 148 patients," *The Journal of Thoracic and Cardiovascular Surgery*, vol. 121, no. 5, pp. 842–853, 2001.

[3] M. Joinie-Maurin, B. Bayle, and J. Gangloff, "Force feedback teleoperation with periodical disturbance compensation," in *2011 IEEE International Conference on Robotics and Automation (ICRA) Proceedings*, may 2011, pp. 4828 –4833.

[4] O. A. J. van der Meijden and M. P. Schijven, "The value of haptic feedback in conventional and robot-assisted minimal invasive surgery and virtual reality training: a current review," *Surgical Endoscopy*, vol. 23, pp. 1180–1190, 2009.

[5] H. Mayer, I. Nagy, A. Knoll, E. U. Braun, R. Bauernschmitt, and R. Lange., "Haptic feedback in a telepresence system for endoscopic heart surgery," *MIT Presence: Teleoperators and Virtual Environments*, vol. 16, No5, pp. 459–470, 2007.

[6] M. Mitsuishi, N. Sugita, and P. Pitakwatchara, "Force-feedback augmentation modes in the laparoscopic minimally invasive telesurgical system," *Mechatronics, IEEE/ASME Transactions on*, vol. 12, no. 4, pp. 447 –454, aug. 2007.

[7] K. Onda, T. Osa, N. Sugita, M. Hashizume, and M. Mitsuishi, "Asynchronous force and visual feedback in teleoperative laparoscopic surgical system," in *Intelligent Robots and Systems (IROS), 2010 IEEE/RSJ International Conference on*, oct. 2010, pp. 844 –849.

[8] T. Yamamoto, B. Vagvolgyi, K. Balaji, L. L. Whitcomb, and A. M. Okamura, "Tissue property estimation and graphical display for teleoperated robot-assisted surgery," in *Robotics and Automation, 2009. ICRA '09. IEEE International Conference on*, may 2009, pp. 4239 –4245.

[9] A. Achhammer, C. Weber, A. Peer, and M. Buss, "Improvement of model-mediated teleoperation using a new hybrid environment estimation technique," in *2010 IEEE International Conference on Robotics and Automation (ICRA)*, may 2010, pp. 5358 –5363.

[10] P. Boonvisut and M. C. Cavusoglu, "Estimation of soft tissue mechanical parameters from robotic manipulation data," *Mechatronics, IEEE/ASME Transactions on*, vol. PP, no. 99, pp. 1 –10, 2012.

[11] R. Howe, W. Peine, D. Kantarinis, and J. Son, "Remote palpation technology," *Engineering in Medicine and Biology Magazine, IEEE*, vol. 14, no. 3, pp. 318–323, 1995.

[12] A. Talasaz and R. Patel, "Remote palpation to localize tumors in robot-assisted minimally invasive approach," in *Robotics and Automation (ICRA), 2012 IEEE International Conference on*, 2012, pp. 3719–3724.

[13] M. Mitsuishi, M. Hashizume, P. Navicharern, Y. Fujino, K. Onda, S. Yasunaka, N. Sugita, J. Arata, H. Fujimoto, K. Tanimoto, K. Tanoue, S. Ieiri, K. Konishi, and Y. Ueda, "A telesurgery experiment between japan and thailand," in *The 6th International Conference on Ubiquitous Robots and Ambient Intelligence (URAI 2009)*, 2009.

[14] J. Arata, H. Takahashi, P. Pitakwatchara, S. Warisawa, K. Tanoue, K. Konishi, S. Ieiri, S. Shimizu, N. Nakashima, K. Okamura, Y. Fujino, Y. Ueda, P. Chotiwan, M. Mitsuishi, and M. Hashizume, "A remote surgery experiment between japan and thailand over internet using a low latency codec system," in *2007 IEEE International Conference on Robotics and Automation (ICRA),*, April 2007, pp. 953–959.

[15] R. E. Kalman, "A new approach to linear filtering and prediction problems," *Transactions of the ASME–Journal of Basic Engineering*, vol. 82, no. Series D, pp. 35–45, 1960.

[16] N. Dioiaiti, C. Melchiorri, and S. Stramigioli, "Contact impedance estimation for robotic systems," in *Intelligent Robots and Systems, 2004. (IROS 2004). Proceedings. 2004 IEEE/RSJ International Conference on*, vol. 3, sept.-2 oct. 2004, pp. 2538 – 2543 vol.3.

[17] A. Haddadi and K. Hashtrudi-Zaad, "Real-time identification of hunt-crossley dynamic models of contact environments," *Robotics, IEEE Transactions on*, vol. 28, no. 3, pp. 555 –566, june 2012.

[18] F. Lalys, L. Riffaud, D. Bouget, and P. Jannin, "A framework for the recognition of high-level surgical tasks from video images for cataract surgeries," *Biomedical Engineering, IEEE Transactions on*, vol. 59, no. 4, pp. 966 –976, april 2012.

[19] N. Padoy, B. Tobias, H. Feussner, M.-O. Berger, and N. Navab, "On-line recognition of surgical activity for monitoring in the operating room," in *20th Conference on Innovative Applications of Artificial Intelligence - IAAI'08*, Chicago, États-Unis, 2008, pp. 1718–1724. [Online]. Available: http://hal.inria.fr/inria-00331390

[20] S. Voros and G. Hager, "Towards "real-time" tool-tissue interaction detection in robotically assisted laparoscopy," in *Biomedical Robotics and Biomechatronics, 2008. BioRob 2008. 2nd IEEE RAS EMBS International Conference on*, oct. 2008, pp. 562 –567.

[21] H. C. Lin, I. Shafran, T. E. Murphy, A. M. Okamura, D. D. Yuh, and G. D. Hager, "Automatic detection and segmentation of robot-assisted surgical motions," in *Proceedings of the 8th international conference on Medical Image Computing and Computer-Assisted Intervention - Volume Part I*, ser. MICCAI'05, 2005, pp. 802–810.

[22] C. Cortes and V. Vapnik, "Support-vector networks," *Machine Learning*, vol. 20, pp. 273–297, 1995.

[23] A. Aizerman, E. M. Braverman, and L. I. Rozoner, "Theoretical foundations of the potential function method in pattern recognition learning," *Automation and Remote Control*, vol. 25, pp. 821–837, 1964.